Since January 2020 Elsevier has created a COVID-19 resource centre with free information in English and Mandarin on the novel coronavirus COVID-19. The COVID-19 resource centre is hosted on Elsevier Connect, the company's public news and information website.

Journal of Transport Geography 99 (2022) 103265

Contents lists available at ScienceDirect

Journal of Transport Geography

journal homepage: www.elsevier.com/locate/jtrangeo

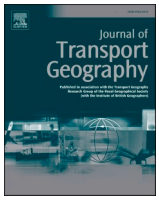

Global shipping network dynamics during the COVID-19 pandemic's initial phases

Christopher Dirzka, Michele Acciaro *

Department of Operations and Technology, Kühne Logistics University (KLU), Hamburg, Germany

ARTICLE INFO

Keywords:
Pandemic disruption
Network analysis
Liner shipping network dynamic
Public notices

ABSTRACT

Catastrophic incidents can significantly disrupt supply chains, but most of these disruptions remain localized. It was not until the onset of COVID-19 that a disruption in our lifetimes achieved a global magnitude. In order to contain the pandemic, governments around the world resorted to closing borders, shutting down manufacturing plants, and imposing lockdowns, which resulted in disrupted production capabilities and weakened consumer spending. The effects of these measures have been clearly visible in global transport networks, where disruptions ripple through the system and serve as a precursor to the disruptions in the broader economy. In this study, we use liner shipping schedule cancellations, a form of serious transport network disruption, as distress signals of the pandemic's impact on global supply chains. Our study applies a three-stage approach and provides insights into operator behaviors when under distress. We show that the pandemic challenged service network integrity and that network disruptions first clustered in Asia before rippling along main trade routes. Agile liner shipping operations, aided by planned service suspensions, prevented the collapse of the global maritime transport networks and indicated the maritime industry's ability to withstand even major catastrophic incidents.

1. Introduction

Disasters are generally localized and seldom reach global proportions. However, the pneumonia cases first reported by China's Wuhan Municipal Health Commission on the 31st December 2019 caused a global emergency that can be characterized as a catastrophic incident.[1] The novel coronavirus and its accompanying disease, COVID-19, were declared a pandemic in March 2020 (WHO, 2020). In April 2020, the Sustainable Development Group, a United Nations organization, concluded that the '*COVID-19 pandemic is far more than a health crisis: it is affecting societies and economies at their core*' (UNSDG, 2020 p.3).

In the attempt to contain the virus, countries resorted to temporary border closings, manufacturing plant shutdowns, and mandated social distancing (i.e., a risk-mitigation strategy to lessen human interactions) (De Vos, 2020; Hotle et al., 2020). Such measures impacted supply and constrained global consumer demand (World Economic Forum, 2020). The pandemic's geographical spread started in mainland China, the World's manufacturing hub, and quickly impacted global importers—depleting stocks and significantly impacting transport networks (Ivanov, 2020).

Since the onset of the pandemic, a rich literature has emerged regarding the impact of this catastrophic incident on transport networks and operations. Initial research highlighted the impact of the pandemic on local networks, most notably on public transport and leisure travel (De Vos, 2020; Borkowski et al., 2021; Chang et al., 2021; Wang et al., 2021). As the pandemic spread across international boundaries, research started to focus on the passenger and cargo air transport industries (e.g., Bombelli, 2020; Sobieralski, 2020; Suau-Sanchez et al., 2020).

Similarly, research in the shipping industry initially focused on the cruise segment, which was heavily affected at the beginning of the crisis because of high on-board infection rates and eventually had to halt operations completely (e.g., Gilmour et al., 2020; Ito et al., 2020). The cargo shipping segments did not sustain a complete network breakdown, but were nonetheless heavily disrupted.

Seminal studies (e.g., Verschuur et al., 2021; March et al., 2021; Zheng et al., 2021; Guerrero et al., 2022), which were primarily based

* Corresponding author.
E-mail addresses: Christopher.Dirzka@the-klu.org (C. Dirzka), Michele.Acciaro@the-klu.org (M. Acciaro).

[1] According to the Federal Emergency Management Agency's (FEMA) National Response Framework, catastrophic incidents refer to human-made or natural incidents that impact the population, economy, infrastructure, or governance structures. In such cases, the distress exceeds available resources and mandates an emergency response (https://www.fema.gov/).

https://doi.org/10.1016/j.jtrangeo.2021.103265
Received 4 June 2021; Received in revised form 2 December 2021; Accepted 11 December 2021
Available online 18 December 2021

on ship position and ship status information, confirmed how shipping networks were affected during the pandemic's initial phases. However, these studies were unable to identify patterns in the disruptions. Disruptions occurred for various reasons, ranging from the difficulty in performing crew changes to port restrictions, but also to the sudden reduction in consumer demand and the collapse of industrial production in many parts of the world (United Nations, 2021). These disruptions resulted in shipping network changes.

In contrast to other shipping networks (e.g., tramp or industrial shipping), liner shipping operates on fixed schedules (i.e., liner services), which constitute the service networks that are designed to be scalable and interconnected. Correspondingly, these networks are vulnerable to cascading failures, as a disruption in one node in the call sequence impacts subsequent nodes. Due to this characteristic, liner shipping networks can carry a distress signal once disruptions occur. In order to develop robust responses to future catastrophic incidents and design resilient networks, it is crucial to understand the network dynamics during the pandemic's initial phases.

So far, the literature has only paid limited attention to pandemic-related service network dynamics in an industry like liner shipping. In a series of contributions, (Ivanov et al., 2014; Dolgui et al., 2018, 2020; Ivanov and Dolgui, 2021) investigated transport network disruptions and identified cascading failures (also referred to as the ripple effect) as a structural dynamic involving a downstream disruption propagation. Contrary to the more commonly discussed bull-whip effect, the ripple effect is a low-frequency and high-impact supply chain disruption. However, this concept has not been applied to service network designs. Its application would allow one to capture a disruption type as it happens in liner shipping, where affected nodes impact successive nodes in a service call sequence. The operations research literature (i.e., Brouer et al., 2013; Li et al., 2015, 2016) has proposed theoretical frameworks for modeling impaired calls and the subsequent propagation effects, but none have been complemented by empirical investigations of cascading failures in ocean shipping networks.

Against that background, the present research poses and explores this question: '*to what extent and in which manner has the pandemic impaired liner shipping networks?*' We study operational behavior under distress within network structures, shedding light on whether disruptions cluster in geographical areas and ripple effects materialize. Our goal is to illuminate the factors behind disruption dynamics and global service networks. To this end, we used liner shipping schedule cancellations—a form of serious transport network disruption and a type of distress signal by liner operators—to capture disruption dynamics.

Our study proposes a three-stage design that relies on network theory and simulation. The proposed methodology is based on public notices issued by liner operators during the pandemic's initial phases from January to May 2020. Such notices are published on the operator's website to warn shippers that a service can not be provided as indicated in the liner schedule. This information is represented graphically to not only visualize the network disruption, but also apply network theoretical indicators to measure shifting network dynamics. In addition, we benchmark the disrupted network against a simulated one to identify cascading failures.

Our work contributes to transport geography research, and in particular, the relationship between transport networks and global network disruptions caused by catastrophic incidents. We show that, although network connectivity was persevered, the pandemic imposed a gradually intensifying shock to some geographical clusters that emanated from a local disruption. In addition, this study pioneered the usage of public notices as a way for researchers to better embed qualitative information in future studies of network dynamics. Furthermore, this study provides various theoretical contributions to the transport geography and disruption management literature. This is, in fact, the first study to examine global disruption clustering in liner shipping networks, as well as utilize a novel simulation-based benchmark index to quantify the ripple effect.

The remainder of the paper proceeds as follows: Section 2 examines the literature on disruption types and disruption management in liner shipping. Section 3 presents our process sequence, methods, and relevant metrics for capturing the pandemic's disruption impact. In addition, the section describes the data sourcing and filtering process. Section 4 visualizes global disruptions and analyzes network aspects. Section 5 covers the theoretical and managerial implications of our findings. Section 6 outlines the limitations of our study and illuminates future research avenues.

2. Literature review

Our study primarily relates to research in transport geography and disruption management. Within these domains, we first reviewed the literature on disruptions in ocean shipping networks; secondly, we examined the measures proposed to mitigate the disruption impacts. Given our focus on the pandemic's initial phases, we paid particular attention to ad hoc responses to distress signals in the network. Note that the subsequent review presents the conceptual background, while the relevant methodological issues are discussed in the methodology section (Section 3) in order to avoid duplication and highlight this study's methodological novelty.

2.1. Disruption types in shipping networks

Shipping networks enable high supply chain performance, but are vulnerable to disruptions arising from asset failures, congestion, adverse weather conditions, geopolitical turmoil, or natural disasters (Earnest et al., 2012). Disruptions interfere with the service schedule and translate into diminished product value and trade options (Calatayud et al., 2017). Overall, 47% of ocean shipping voyages are impacted by these schedule deviations (i.e., 53% of voyages arrive according to schedule; Notteboom and Vernimmen, 2009). Indeed, most disruptions are the result of common operational issues, such as congestion and mechanical failures; only a few disruptions have been caused by black swan events, such as terrorist attacks, extreme weather events, and other catastrophic incidents. As a consequence, most scholarly contributions on disruptions in the maritime sector have focused on common operational issues (e.g., Brouer et al., 2013; Qi, 2015).

Disruptions in ocean transportation can be classified into regular and irregular occurrences. The first classification includes instances—such as congestion in the passageways/ports or asset failures—that can be managed through an Operational Control Center (OCC) that coordinates real-time decisions (Brouer et al., 2013). The OCC assesses the risk (e.g., the risk that cargo is hindered from passing through the transport network) and manages potential adverse consequences. Operators' risk awareness and ability to quantify risk allows firms to generally estimate congestion and waiting times and thus schedule recovery time (e.g., Wang and Meng, 2012; Li et al., 2015, 2016). The second classification includes extreme weather conditions, geopolitical turmoil, or natural disasters. The disruptive Fukushima disaster (Dolgui et al., 2018), Hurricane Sandy (Verschuur et al., 2020) or the Suez blockage in 2021 fit into this category—and now, so does the COVID-19 pandemic.

Discussing such disruptions, Wu et al. (2019) investigated the extreme case of maritime channel interruptions. The vulnerability analysis showed that those occurrences would significantly raise voyage length due to the high dependency on these chokepoints Ducruet (2016) in network designs. Earnest et al. (2012) simulated disruptions to the

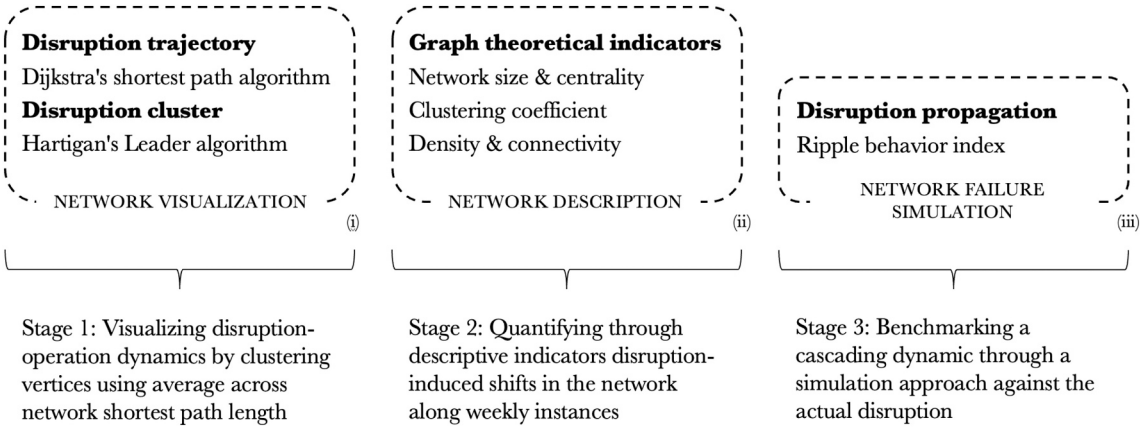

Fig. 1. Methodology process.

trade network by an unspecified terrorist attack in order to evaluate network weaknesses and resilience. The results indicated a negative relation between efficiency and robustness (vice versa for efficiency and resilience). Rousset and Ducruet (2020) used three case studies (the Hanshin-Awaji earthquake, the 9/11 World Trade Center attack and Hurricane Katrina) to analyze irregular occurrences with an exogenous shock that significantly impacted maritime infrastructures, similar to COVID-19. The cases illustrate the adverse impact of catastrophic events on interlinked structures close to the source of disruption, while further away structures are less affected or even serve as backup systems (i.e., showcasing higher economic activity). Another case study, which assessed the destruction of the port of Kobe in 1995 due to an earthquake, presented similar results (i.e., in the post-earthquake period, interlinked ports with Kobe were able to gain traffic) (Kosowska-Stamirowska, 2020).

Due to the pandemic's unique disruption risks and exogenous nature—a local source spreading to adjunct networks (Ivanov, 2020; Ivanov and Dolgui, 2020)—it is critical that liner operators utilize ad hoc responses to avoid a network breakdown. The subsequent section outlines an array of mitigation strategies that have been observed in practice.

2.2. Disruption response in liner shipping

Shipping networks' response to distress depends on the disruption's severity and duration. Operators respond to severity and duration at various hierarchical levels (i.e., strategic adjustments to the fleet, alliance membership or network design, tactical adjustments routing and scheduling, or operational adjustments to cargo commitments).

In reference to a disruption's initial phases, this study reviews operational adjustments to network dynamics. Operational responses refer to crew scheduling, ad hoc ship rescheduling, cargo booking, or cargo routing. Service pricing, managing cargo, and handling sudden occurrences are governed under a short-term horizon (Pesenti, 1995; Christiansen et al., 2004; Agarwal and Ergun, 2008).

As a response on the operational level, operators can cancel a service commitment by either canceling or omitting a port call. But this generates another disruption source, such as causing network connectivity problems for the liner operator and interrupting the shippers' just-in-time planning schedules. Thanks to parallel lines on critical services (Lam and Yap, 2011), rolled cargo (i.e., cargo that has not been loaded onto the vessel it was meant to sail on) is then picked up under another service at the same berth in the next service cycle. Liner operators within alliances can use horizontal inter-organizational flexibility to roll cargo to other members (Mason and Nair, 2013a,b). An alternative means of avoiding rolling cargo is to defer a ship's departure (Brouer et al., 2013). It should be noted that in liner shipping, there are no penalties associated with rolled cargo, as contractual agreements do not generally cover shipper penalties imposed on operators for schedule deviations (Fransoo and Lee, 2013).

With reference to the impact of COVID-19 on ocean transportation, most liner shipping operators cancelled service commitments during the pandemic's initial phases—first in response to the operational disruptions caused by the pandemic and then due to dwindling demand. The idle capacity was laid up in anchorage and vessels were diverted on longer routes (i.e., avoiding the Suez Canal and favoring the journey around the Cape of Good Hope) in an attempt to reduce operational capacity and maintain higher ship utilization rates, which are at the core of any carrier's bottom line (Pooler, 2020; Pooler and Hale, 2020).

In sum, this review illustrates the different disruption types that occur in liner shipping, as well as the adhoc disruption management responses in liner shipping networks. The following section outlines the information set used to construct the network and the three-stage approach used to investigate ad hoc ship rescheduling.

3. Research design, data description and methodology

3.1. Research design

The objective of our work is to provide insights into the disruptions caused by COVID-19 during the pandemic's initial phases and study their network effects using public notices. Given the limited amount of research on catastrophic incidents in liner shipping, and the absence of any study linking catastrophic incidents to public notices, our study is an

exploratory analysis that combines qualitative and quantitative methods. Our research design makes use of visual and descriptive approaches along with network benchmarking metrics, as well as quantifies the ripple effect by means of a benchmark with a simulated network. We designed a three-stage research approach as outlined in Fig. 1. Our research approach is hence based on (i) visualizing disruption dynamics by reconstructing disrupted service trajectories and clustering impacted onshore infrastructure; (ii) providing descriptive insights into network shifts along the observation horizon; and (iii) constructing a simulation-based benchmark index to identify how failures cascade along the network. As our research is built on data that has been analyzed for the first time, it is expedient to illustrate the characteristics of the data and how various databases have been combined before providing the details of each method.

3.2. Data description

This study utilizes liner operators' public notices (so-called *blank sailing notices*) and operational liner shipping schedules. This information enabled us to map the disrupted and undisrupted network (i.e., the network that remained operational according to schedule). Since public notices show suspended services, they can be used to assess operations under distress. Such an information set overcomes the drawbacks associated with the use of high-frequency information, such as Automatic Identification System data, which indicates ship position but omits references to the actual operational state or cause of idling (March et al., 2021; Verschuur et al., 2021; Zheng et al., 2021; Guerrero et al., 2022).

Liner schedules are similar to a bus itinerary. The schedule establishes a call sequence, defines the intervals between calls, and assigns resources to service the operation. The customers to be served are notified (in the liner shipping case, several months ahead) so that production can be managed. The information sharing between ocean carriers, logistics providers and shippers is critical for supply chain foresight and a fundamental enabler of global supply chain relations. Although liner shipping operations can refer to the transport of various types of cargo, the term is primarily used as a synonym for container shipping. In this sector, most operations are carried out under a schedule, in contrast to tramp shipping (where ships seek available cargoes without a fixed itinerary) or industrial shipping (in which ships and cargo are owned by the same stakeholder) (see Christiansen et al. (2004, 2013, 2020) for a discussion of the differences among these types of shipping).

In cases where a schedule disruption occurs as a result of a node becoming inaccessible within the call sequence (whether due to operational reasons or even a lack of cargo), the ship operator issues a public notice so that cargo owners have an opportunity to reevaluate their logistic chain decisions. Against this background, public notices or blank sailings refer to the liner operator's ad hoc decision to cancel a service commitment. Rescheduling or cancelling a service is a common tool that operators use to reduce operational supply and achieve better capacity utilization, and thereby maintain service competitiveness and protect their bottom line.

Most rescheduling does not cause major disruptions: During holiday periods, for example, cargo demand is lower than usual, and hence services can be rescheduled or cancelled with only limited cargo rolling. During the Chinese New Year, for example, offices and manufacturing plants shut down across China. Migrant workers in the coastal regions return to their rural homes, leaving logistic centers understaffed and contributing to a reduction in transportation service capacity. This causes global trade volumes to diminish, and ship operators respond by issuing blank sailings, corresponding capacity-wise to on average 2*mil*. *TEU* or 94 ultra-large container ships with each able to carry 21,000 TEUs (DHL, 2021). While disruptions such as the Chinese New Year are foreseeable, other disruptions such as those caused by extreme weather events, emergency maintenance, or catastrophic incidents also drive ocean carriers to adjust operations.

Table 1
Raw network illustration.

Type	Case
Sequence	CNTAO → CNSHA → CNNGB → KRPUS → USLGB → USOAK
Path length	[393, 139, 498, 5465, 376]
Carrier	MSC
Service	ORIENT
Direction	EB
Class	cancelled
Week	2020-04-27 - 2020-05-03

Note: Network nodes and links are based on the service call sequence (UN/LOCODE). Voyages length in nautical miles (nm) within the sequence are estimated based on a shortest path algorithm. Services split among eastbound, westbound, eastbound and northbound direction. Binary class indicator flags *in-operation* and *cancelled* services. Scaling based on weekly observations.

Public notices are published on the carrier's website or other communication channels. They typically include information about the impacted service code and the duration of the service commitment cancellation. The following is an example of such public notices:

'*Europe - Middle East & Indian Subcontinent Blank Sailing Announcement…April 6 2020…In relation to ('reason'), we have seen a significant reduction in demand…blank sailings between ('X') service…*'[2]

In this study, we constructed a baseline network using liner schedules (i.e., operated services) that are publicly available for all major carriers alongside public notices (i.e., cancelled services). The dataset was gathered via online databases maintained by ocean information providers that specialize in container tracking (Ocean Insights, 2020) and sailing schedules (Linescape, 2020). Moreover, any notices sourced via the online database were cross-checked against the liner operators' own public statements. Overall, the samples include 11 different liner operators[3] with 221 unique suspended service codes (or 1440 overall service codes) and scaled on weekly basis {1, 2, …, 22}, i.e., 30th December 2019 until 31 st May 2020. Liner operators in the sample operated 82.35% (share in TEU capacity) in Q1 2020 and carried out most ocean shipping services.

The sampled data are structured in a similar manner, and include information on the liner operator, the service code and direction, and the service sequence along the weekly schedule. We used the services codes and direction as indices to merge the sailing schedules and public notices in order to produce the raw information used in our analysis. A data entry example is provided in Table 1.

The call sequence includes multiple voyages. Individual voyages link the nodes, which are captured by a unique code, i.e., United Nations Code for Trade and Transport Locations (UN/LOCODE). In the illustration, the first voyage (*CNTAO → CNSHA*) in the call sequence links the Port of Qingdao and Port of Shanghai. Based on the public notice by the operator, this service is cancelled in week 18—an operational service would be classified as '*in-operation*'. Such classification allows us to generate the disrupted and undisrupted networks.

Due to varying or missing inputs by the operators, we included any cancelled service within the aforementioned observation horizon, i.e., we disregarded the underlying cancellation reasons, such as non-working days, capacity adjustments, or pandemic disruption. Besides, we relied on the number of cancelled services as weights rather than cancelled capacity due to lacking insights about the withdrawn capacity

[2] Public access via https://www.maersk.com/news/.

[3] Gathered schedule information includes the liner operators: Mærsk, MSC, CMA-CGM, Evergreen, Hapag-Lloyd, COSCO, APL, OOCL, Yang Ming, Hyundai and ONE Line.

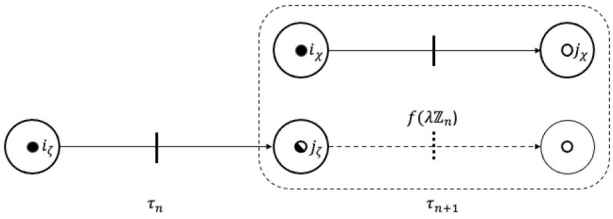

Fig. 2. Network simulation benchmark.

(i.e., capacity which would have been assigned via the schedule, but was withdrawn due to the cancellation).

The network obtainable from the public schedules (i.e., *undisrupted*) includes 626 unique nodes and 4,049 unique links, while the network including the public cancellation notices (i.e., *disrupted*) contains 189 unique nodes and 923 unique links. Each service code (whether disrupted or undisrupted) is associated with eastbound, westbound, southbound, and northbound direction codes. In addition, some service codes are shared by multiple operators with different coverage along a service sequence. Due to this overlap, we refer to a service as a schedule with a unique code, direction, and operator, which results in 605 suspended services.

3.3. Methodology

Network theory allows us to observe the structural relations among nodes and links in a network. It also implies that '*Locations are not unique*' (Bunge, 1966, p. 100) (i.e., nodes in a network possess distinct properties, but are not fundamentally '*like nothing else, singular, indescribable*' (p. 237)). This corresponds to the notion that a node (i.e., port locations in ocean shipping networks) embedded in a structure shares similar features with its neighbors, revealing the interdependence between connected points. Consequently, a disruption pressures liner shipping operators to initially adjust relatively connected network

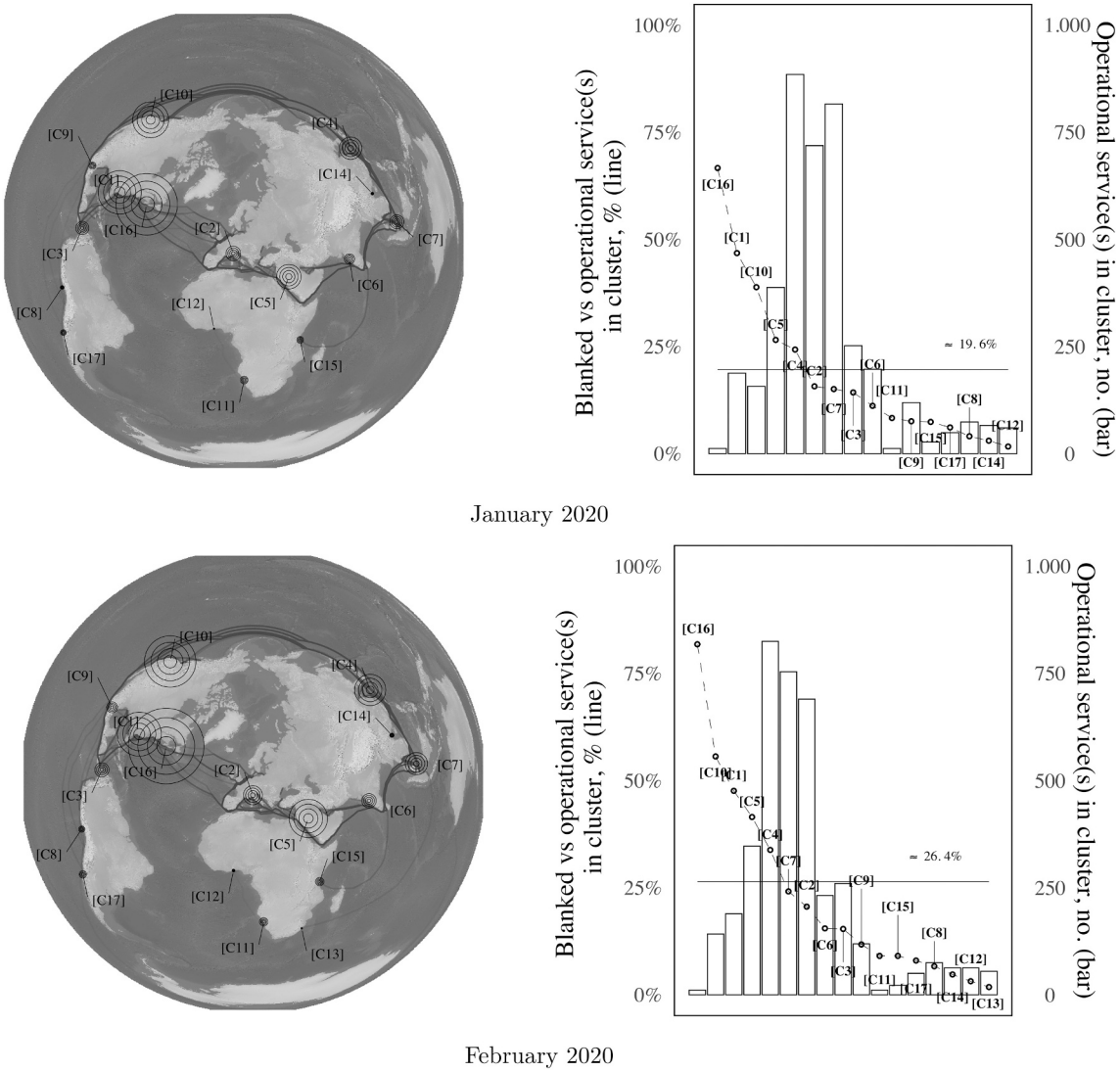

Fig. 3. Blank sailing mapping and cluster - January–May 2020. Note: Weekly blank sailing services transformed to monthly observations. Disrupted trajectories (i, j) are relinked via the Dijkstra's shortest path algorithm. Manual adjustments applied to designate the Northern Sea route as unfeasible solution. Clusters centroids are assigned via Hartigan's Leader algorithm with a fixed radius ($\overline{R} \approx 1774.3$nm), i.e., mean trajectory length in observation horizon. Cluster size aligns with the ratio of blanked sailings to operational services. Maps are displayed using the Lambert azimuthal equal-area projection (World Geodetic System 1984 (WGS84)).

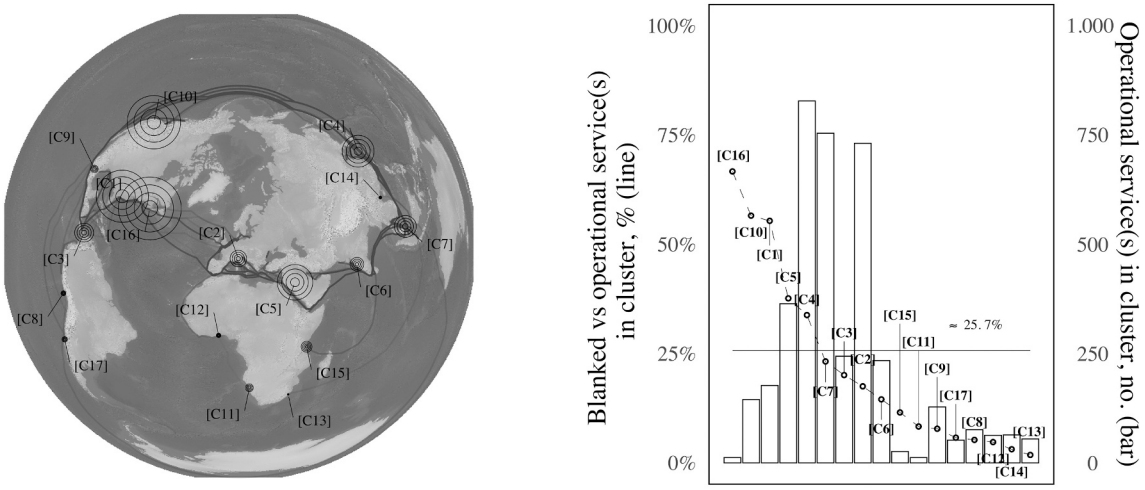

March 2020

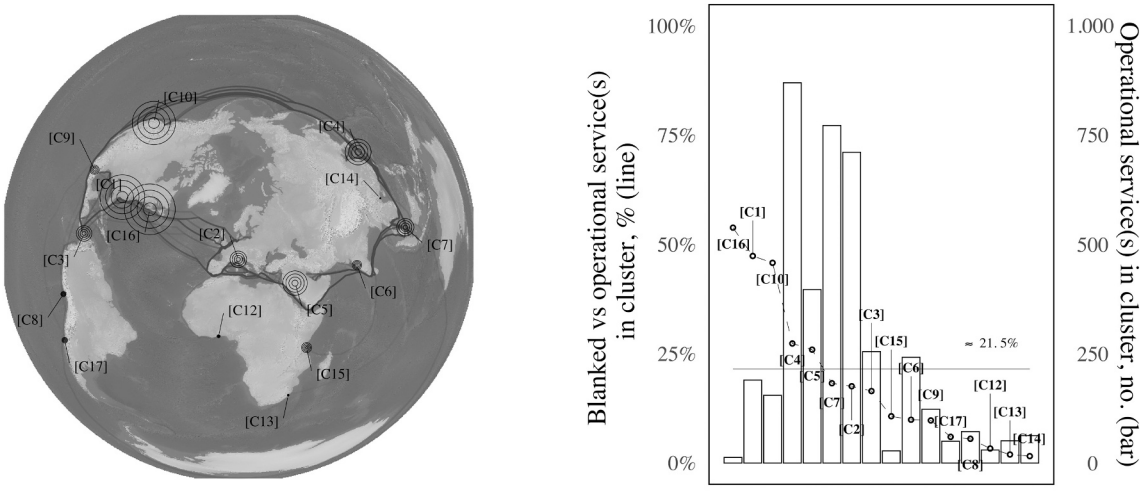

April 2020

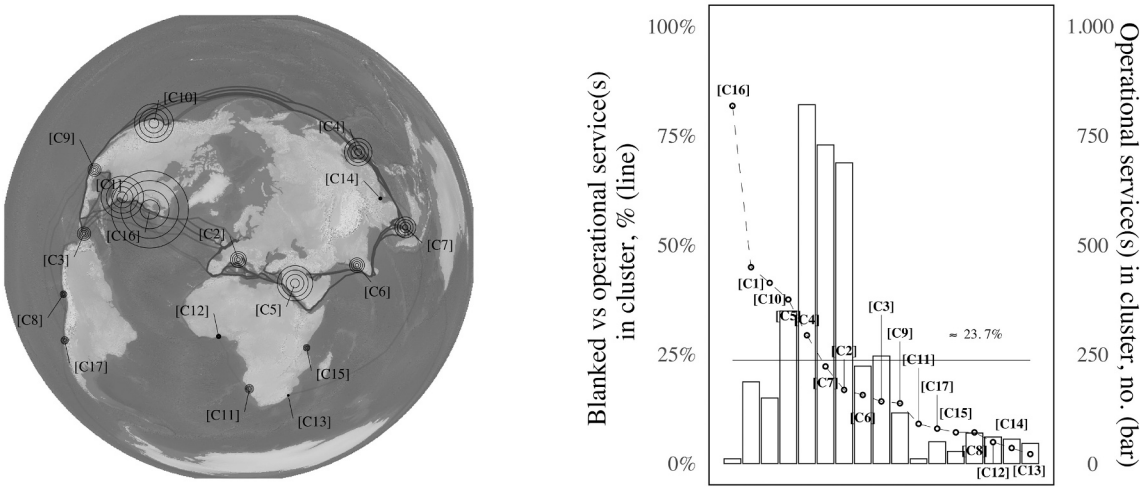

May 2020

Fig. 3. (*continued*).

Table 2
Network analysis.

	January				February				March					April				May				
	1	2	3	4	5	6	7	8	9	10	11	12	13	14	15	16	17	18	19	20	21	22
Descriptive																						
$\sum v$	107	113	103	134	133	126	139	136	154	133	140	145	140	131	130	128	144	128	128	134	134	135
$\sum v/\sum V$	0.18	0.19	0.17	0.22	0.22	0.21	0.23	0.23	0.25	0.22	0.23	0.24	0.23	0.22	0.21	0.21	0.23	0.21	0.21	0.22	0.22	0.25
$\sum e$	309	289	276	390	392	426	464	416	449	418	416	474	411	426	398	412	394	396	429	400	390	400
$\sum e/\sum E$	0.09	0.08	0.08	0.11	0.11	0.12	0.13	0.11	0.12	0.12	0.11	0.13	0.11	0.12	0.11	0.11	0.11	0.11	0.12	0.11	0.11	0.15
$\sum \lambda_v f_v$	940	1033	948	920	726	827	974	906	858	1007	1178	858	965	1067	961	823	936	879	902	703	866	849
$\sum \lambda_V f_V$	503	496	497	497	516	500	491	503	497	489	483	492	493	483	490	496	492	484	484	479	466	454
Indices																						
$\varnothing_n$	16	13	16	13	13	13	13	14	15	12	16	16	13	11	14	11	14	13	16	12	18	12
$\varnothing_n/\varnothing_N$	1.14	0.93	1.14	0.93	0.93	0.87	0.87	1	1.07	0.8	1.14	1.14	0.87	0.73	0.93	0.79	0.93	0.87	1	0.86	1.2	0.75
β_n	2.89	2.56	2.68	2.91	2.95	3.38	3.34	3.06	2.92	3.14	2.97	3.27	2.94	3.25	3.06	3.22	2.74	3.09	3.35	2.99	2.91	2.96
β_n/β_N	0.5	0.43	0.45	0.48	0.49	0.56	0.56	0.51	0.49	0.53	0.5	0.55	0.49	0.55	0.51	0.55	0.46	0.52	0.57	0.52	0.51	0.62
γ_n	0.03	0.02	0.03	0.02	0.02	0.03	0.02	0.02	0.02	0.02	0.02	0.02	0.02	0.03	0.02	0.03	0.02	0.02	0.03	0.02	0.02	0.02
γ_n/γ_N	2.79	2.32	2.66	2.19	2.25	2.74	2.45	2.27	1.95	2.41	2.18	2.33	2.14	2.55	2.41	2.63	1.98	2.48	2.69	2.36	2.32	2.54
C_{D_n}	0.09	0.13	0.08	0.1	0.1	0.17	0.13	0.12	0.12	0.12	0.15	0.16	0.13	0.17	0.13	0.12	0.1	0.13	0.1	0.13	0.15	0.16
C_{D_n}/C_{D_N}	0.73	1.05	0.64	0.74	0.76	1.35	0.97	0.88	0.94	0.93	1.2	1.28	0.98	1.39	1.05	1.01	0.82	1.08	0.81	1.08	1.26	1.47
C_{B_n}	0.25	0.43	0.2	0.27	0.25	0.4	0.29	0.28	0.34	0.22	0.33	0.35	0.31	0.37	0.29	0.27	0.27	0.31	0.21	0.35	0.3	0.37
C_{B_n}/C_{B_N}	1.17	1.89	0.83	1.16	1.04	1.86	1.27	1.21	1.56	0.89	1.48	1.57	1.29	1.77	1.37	1.22	1.18	1.35	0.88	1.44	1.4	1.66
$C(g)_n$	0.29	0.21	0.23	0.25	0.26	0.26	0.27	0.27	0.27	0.26	0.28	0.28	0.27	0.25	0.28	0.26	0.28	0.24	0.29	0.26	0.25	0.23
$C(g)_n/C(g)_N$	1.15	0.84	0.91	1	1.01	1.06	1.09	1.07	1.06	1.04	1.11	1.12	1.08	0.99	1.12	1.02	1.12	0.97	1.13	1.03	1.01	0.97
$C(l)_n$	0.31	0.23	0.27	0.29	0.32	0.33	0.33	0.32	0.3	0.31	0.32	0.38	0.35	0.34	0.32	0.35	0.34	0.27	0.3	0.29	0.35	0.35
$C(l)_n/C(l)_N$	0.69	0.49	0.58	0.63	0.69	0.71	0.72	0.7	0.65	0.68	0.7	0.83	0.77	0.75	0.7	0.77	0.73	0.58	0.64	0.66	0.77	0.82
Simulation																						
L_B	NA	0.34	0.34	0.36	0.41	0.38	0.39	0.42	0.42	0.37	0.46	0.41	0.43	0.47	0.46	0.38	0.39	0.39	0.46	0.41	0.43	0.45
U_B	NA	0.21	0.21	0.29	0.26	0.28	0.29	0.28	0.28	0.25	0.28	0.28	0.26	0.27	0.27	0.27	0.27	0.25	0.3	0.26	0.26	0.33

Note: Overall distinct disrupted vertices ($\sum v$) and edges ($\sum e$) with benchmark against undisrupted structures, represented as a fraction ($\sum v/\sum V$, *sum e/sum E*). Shortest path in nautical miles for undisrupted and disrupted vertices as weigthed mean ($\sum \lambda f$), i.e., based on path frequency (f). Diameter is the length of the shortest path between the most distant nodes, i.e., disrupted network ($\varnothing_n$ and as benchmark $\varnothing_n/\varnothing_N$). Beta index accounts for network complexity (β_n and as benchmark β_n/β_N). Gamma Index measures connectivity (γ_n and as benchmark γ_n/γ_N). Degree and betweenness centrality index for the disrupted network captured by C_D and C_B, including respective benchmarks. Transitivity (global) ($C(g)$) refers to the overall clustering coefficient and transitivity (local) ($C(l)$) describes the average clustering coefficient.

structures and focus on distant ones at a subsequent stage. Once an ocean carrier adjusts its service, a distress signal is dispatched along the network.

This study renders these distress signals into a network representation, which allows us to characterize the network's size (overall vertices and edges), complexity (i.e., overall nodes and links ratio), connectivity (i.e., overall connectivity), centralization (overall node importance), and clustering (i.e., community structures). A simulated benchmark, which reconstructs the disrupted network and remaining operations within the network along the observation horizon, allows us to generate insights into the degree and dynamic of the disruption.

The visualization and descriptive network analysis stages (i-ii) align with standard network analysis approaches in transportation science (Ducruet, 2020). In ocean network research, these approaches have become common practice due to available high-frequency information (Ducruet et al., 2010). As an illustration, a network analysis approach has been used to evaluate global maritime structures (Ducruet and Notteboom, 2012b), trade flows (Ducruet, 2013), onshore infrastructure networks (Ducruet and Notteboom, 2012a; Wang and Cullinane, 2016), or vulnerabilities in liner shipping networks (Calatayud et al., 2017). Ducruet and Beauguitte (2014) and Borgatti (2005) provided a thorough review of network analysis techniques and applications. The network simulation stage (iii) proposes a network theory simulation approach to examine the manner the global disruption impaired links in the liner network. Such an approach joins network theory (i.e., structural relations) and an iterative simulation method. The framework relies on prior works concerning disruption propagation and interdependent networks (e.g., Crucitti et al., 2004; Wu et al., 2007; Tang et al., 2016).

3.3.1. Network visualization

The visualization stage serves to provide a geographical perspective on the liner shipping network disruption. In order to reconstruct suspended service trajectories, we solve a shortest path problem to link the impaired vertices (i, j). Based on the gathered public notices, which include the service code and cancelled service sequence, we join each vertex in the sequence with its geographical coordinates $i_{[long,lat]} \rightarrow j_{[long,lat]}$. Dijkstra's algorithm is a classical dynamic programming approach to solve such a problem (Dijkstra, 1959). Given a raster projected as graph $G = (V, E)$ with respective vertices (V) and edges (E), the shortest path along a source node i and sink node j is iteratively estimated until an optimal solution is achieved. As an illustration: The Westbound Asia to Europe service is cancelled, which includes the voyage - Felixstowe (GB) to Rotterdam (NL). A linear path linking these nodes would yield the shortest path, intersecting landmasses (i.e., unfeasible paths for waterway transportation). To visualize these cancelled voyages, we initially deemed direct (i.e., tangent landmasses) or unrealistic trajectories (i.e., Northern Sea route) as unfeasible. We then generated a rasterized map that only included feasible intersections with an edge cost ($c(e) = 1$). The cost to traverse along $i\rightarrow$ to the next intersection is estimated until all paths options are exhausted, and the shortest path to j based on the lowest edge cost is selected.

Subsequently, we applied Hartigan's Leader algorithm (Hartigan, 1975) to the whole network. Such an algorithm is suitable to clusters' geographical points based on a fixed radius (R) and larger data sets thanks to fast convergence. Notably, we chose to use the average distinct trajectory length along the observation horizon, i.e., $\overline{R} \approx 1774.3$nm. Through clustering, one can uncover '*possible small worlds or strongly interconnected components*' (Ducruet et al., 2010, p. 513), i.e., onshore infrastructure in proximity. By combining this data with information about disrupted services, which intersect these clusters, we can estimate the regional impact. Note that a *service* refers to the unique operators, service registration and direction code. Cluster sizes are proportional to the benchmark index $|D_{c_{\tau_n}}|/|S_{c_{\tau_n}}|$, where $|D_{c_{\tau_n}}|$ are disrupted services and $|S_{c_{\tau_n}}|$ are all services in the respective cluster c at observation period τ_n, so that cluster sizes show the size of the disruption relative to the size of the cluster.

3.3.2. Network description

The descriptive analysis stage is similar to the structure proposed by works such as Ducruet and Notteboom (2012b) or Calatayud et al. (2017). In contrast to prior cited works, this study considers time-variant disrupted (D) and undisrupted (S) networks. Our choice of network metric was guided by three objectives: (i) capturing the disruption magnitude, which seeks to estimate the disrupted and undisrupted network size (i.e., to what degree were nodes and links within the transport network affected?); (ii) analyzing network connectivity and centrality in order to provide insights into interrelated/-connected disruption response behavior (i.e., to what degree an impacted link is connected to other impacted links?); and (iii) determining the most impacted network segments (i.e., central hubs or rather the spokes?).

Network size includes the overall vertex ($\sum v$) and edge number ($\sum e$), and weighted mean trajectory distance ($\sum \lambda_v f_v$) with λ_v as the distance in nautical miles. As an illustration, in case $D \ll S$ applies in relation to the overall vertex and edge number, then the disruption can be considered as minor. Vice versa would imply that the disrupted network is significantly larger than the undisrupted network (i.e., just a small segment of the whole network remains in service).

Simple indices encompass network diameter ($\varnothing$) (i.e., shortest path length between the most distant network vertices), Beta index (β) (i.e., overall complexity as links over nodes ratio) and Gamma index (γ) (i.e., absolute connectivity as actual links and possible links). A low $\varnothing$ indicates a more connected network while the opposite applies to the β or γ index. The case $D \ll S$ implies more connectivity and/or that the D network is smaller and less complex.

Complex indices are the overall degree centrality (C_D), betweenness centrality (C_B), local ($C(l)$) and global ($C(g)$) clustering coefficient. As an importance measure, centrality was initially applied to social networks (Freeman, 1978; Fleming and Hayuth, 1994; Borgatti, 2005). The degree centrality C_D refers to the edge number a vertex (i) shares with another vertex (j) with $a_{ij} = 1$ if a direct edge is given, otherwise zero, i.e., $C_D i = \sum_{j=1}^{n} a_{ij}$ —which illustrates a vertex's importance within a network.

The overall degree centrality refers to the $\sum_{C_D}$ of the network vertices, i.e., used in this study as a graph-level centrality index. The betweenness centrality C_B refers to a vertex (i) connecting other vertices on the shortest path (SP), i.e., a path with the smallest edge number. The overall sum of the SP between two vertices (ij) is σ_{ij}, while $\sigma_{ij}(g)$ is the SP number through g, i.e., $C_B(g) = \sum_{i \neq g \neq j \in N} \sigma_{ij}(g)/\sigma_{ij}$ (Calatayud et al., 2017). A single disruption within a network hub and with limited local propagation would suggest a high C_D, while a high C_B implies that more vertices are directly interlinked.

In addition, the transitivity or so-called clustering coefficient is quantified, i.e., overall network to contain adjacent nodes interconnected. This clustering coefficient indicates the presence of communities (or clusters). Global transitivity ($C(g)$) is the ratio between the triangle (i.e., referring to three vertices with three pairs connected —closed triplet) and the triplets (i.e., both open triplet with two pairs and closed triplet). In contrast, local transitivity ($C(l)$) is the ratio between the triangle number and the triplets that are centered on individual vertexes, i.e., showing how close a vertex's neighbors are to being a community. Indicating network interconnectedness, a low coefficient suggests a network with a highly connected hub and less connected immediate neighbors, while a high coefficient can show tight communities with homogeneous structures (Ducruet, 2016). As a point of clarification, a disruption dynamic that aligns with the underlying network (i.e., concentrated on hubs and phasing out on spokes) would yield a ratio closer to one.

3.3.3. Network failure simulation

The cascading simulation stage examines the manner in which the disruption spreads through the liner shipping network. Despite the more

recent shift toward direct voyages (Fransoo and Lee, 2013), liner services are multi-call operations (i.e., transit or/and transshipment voyages within a service). As liner networks are interdependent structures, cancelling a service impacts voyages within the respective service and successive voyages interlinked with the disrupted service. While other services can pick up stranded cargo in the operator's network, capacity constraints pose an additional strain on the network. Ivanov et al. (Ivanov, 2020; Ivanov and Dolgui, 2020) classified this disruption type caused by the pandemic as '*ripple effects*', which refer to a disruption type that causes cascading failures along a logistic chain. Such effects are described as '*the impact of a disruption on SC performance and disruption-based scope of changes in the SC structures and parameters*' (Ivanov et al., 2014, p. 2155) and occur if '*a disruption at a supplier or a transportation link cannot be localised and spreads out to other parts of the SC*' (Ivanov, 2017, p. 2).

Operations research has examined the ripple effect in regard to the liner schedule recovery problem (i.e., Brouer et al., 2013; Li et al., 2015, 2016). Besides the optimization-based methods used to model the ripple effects/cascading failures, the network theory literature stream has proposed various simulation-based approaches.

Such approaches are particularly suitable for modeling network failures due to their ability to cope with time variance. The seminal study by Crucitti et al. (2004) modeled cascading failures by removing nodes. Distressed nodes (i.e., nodes unable to dynamically redistribute capacity) caused a network breakdown, pointing to the importance of robust network designs. Wu et al. (2007) advanced the prior study by incorporating various node removal strategies in a scale-free traffic network (i.e., adding traffic flows to the system until a breakdown occurs), highlighting that failures are underpinned by both structural dependencies and functional overloads. Tang et al. (2016) outlined an interdependent dual network structure and examined time-varying cascading failures using node removal strategies, showing that even a small number of impairing nodes leads to a system collapse. In order to quantify the given failures in a static and dynamic supply chain network, . Sokolov et al. (2016) used a multi-stage process that included graph-theoretical performance indicators, such as connectivity coefficient, complexity and centralization index. Chauhan et al. (2021) studied the relationship between network topologies (i.e., interlinkages with structural features) and cascading failures. Based on a simulated disruption, their study uncovered high robustness and lower resilience under nested networks, while hub disruptions critically challenge these structures.

The prior outlined works are primarily theoretical in nature and lacks an empirical validation of cascading failures (reviews by Dolgui et al., 2018; Llaguno et al., 2021). We used the graph-theoretical simulation frameworks as a basis to design a novel cascading failure index, which inverses the node removal strategy—adding nodes to a simulated set and benchmarking it against a benchmark set. The index's objective is to indicate whether a disruption spread occurred under topological specifications. The spread refers to cascading failures that impacted successive nodes in a network. As indicated in Fig. 2, the network is split into a benchmark and simulation subset in order to enable the validation process.

The successive-distressed nodes are selected using the topological distance (in nautical miles) and underlying dynamic network structure. The first criteria allows us to gain insights into the disruption's reach, i.e., it can be assumed that a node even with a direct link to the disruption is less impacted when it is not in said disruption's proximity. The latter criteria ensures that the dynamic's endogenous conditions are preserved, i.e., selected nodes are based on the underlying network within the given observation frame/simulation step. Using a similarity index (Φ), we iteratively benchmarked the simulated and *true* disruption. The resulting index close to $\Phi = 0$ indicated that no disruption propagation occurred, while a disruption with an unmitigated spread through a network equals $\Phi = 1$ (i.e., cascading failures until the whole interconnected network is impacted). In the pseudocode the proposed approach is outlined.

Pseudocode:. Network simulation benchmark

4. Network analysis results

4.1. Network visualization

Stakeholders started to respond to the disruptions caused by COVID-19 (as a catastrophic incident) on the 27th January, when the Chinese government announced that it would prolong the public holidays to contain the pandemic's spread. Social distancing and production capacity shutdowns resulted in operators publishing blank sailing notices through their communication channels.

We utilized the previously outlined information sets to provide a geographical perspective on the liner shipping net- work disruption as outlined in Fig. 3. Each cluster was assigned to a unique identification code ($cluster = \{1, 2, 3, \ldots, c\}$). Nodes in the clusters are outlined in Table 3 in the Appendix. Shifting network dynamics are visualized by assigning the public notices to their respective observation ranges.

Overall, the pandemic can be split into distinct disruption phases. During the pre-COVID phase, suspended services, in absolute terms, were concentrated in North-Eastern Asia due to the Chinese New Year. Once the pandemic started to evolve, cancellations propagated to transshipment hubs in the Middle East and Singapore and then spread to the Pacific and Atlantic trade lanes.

(i) During the pre-COVID phase in January 2020, seasonal blank sailings were dominant, with retail sales especially dropping in North America as the Chinese New Year preparations unfolded. Particular clusters around North Asia and South-East Asia indicate that most notice issues took place in these areas, subsequently impacting the Panama Canal and the Suez Canal. It is worth noting that the small cluster around the North-American East Coast showed more suspended services than the West Coast.

(ii) Multiple disruption clusters emerged in North-East Asia in February 2020 as a byproduct of the Chinese New Year and the subsequent shutdown of manufacturing plants. The lack of onside staff to move the cargo caused shippers to cancel services. In particular, cancellations impacted ports along the Chinese coastline (Yu, 2020; Saul, 2020), which connect the northern manufacturing hubs with international importers. A surge in canceled services is visible on the North-American West Coast and in Intra-Asia trades, indicating a strong disruption to the Pacific trades.

(iii) A slight recovery is visible in March 2020, which can be attributed to cargo delays in the prior month. Cargo stored on berth in Northern Asia was channeled back into the global supply chain (United Nations, 2021), resulting in fewer suspended services, particularly in the North-America West Coast. In contrast, there was a surge in secondary services bound to South Africa and Latin America.

(iv) In April 2020, blank sailings impacted the service network to a lesser degree, pointing to the weakening of the first pandemic shock and a shift toward the economic one, i.e., the 'interim' period between lockdown and diminishing demand higher up the value chain. The European cluster was distinct in terms of a stabilization on a high distress level.

(v) In May 2020, nearly all clusters saw a multi-source disruption resurgence. It is worth noting that most service suspensions occurred at the end of April until mid-May—an observation shared with the World Bank report (Bank, 2020) on COVID-19 disruptions. While suspended services were still concentrated in Asia, more intermediate trades displayed a disruption, such as in the Indian Sub-Continent, in Central America and in West Africa. Disruption clusters in North America, and to some extent Europe, constitute an outlier. Whether the pattern in Europe could be

Pseudocode: Network simulation benchmark

Step 1. Path options: Multi-dimensional path options ($\mathbb{Z}$) frame is generated. $\mathbb{Z}$ is scaled on a weekly basis as $\tau = \{1, 2, ...22\}$ and contains each unique voyage (i.e., *in-operation* and *cancelled* links). Shortest path (λ) distance linking $\overrightarrow{ij}$ included.

Step 2. Iterative process: *Constructing the disrupted network (χ) in τ_{n+1} —true disruption and its lagged form (ζ) in τ_n —pre-step simulation basis. Both network frames are constrained to cancelled voyages.*

Step 2.1. Simulation process: *Calling ζ and solving the upper- (U_B) and lower bound (L_B): U_B is equal to any path option is selected by voyage end node in ζ_{τ_n} and voyage start node in $\mathbb{Z}_{\tau_{n+1}}$. L_B is equal to the closest path option by voyage end node (j) in ζ_{τ_n} and voyage start node (i) in $\mathbb{Z}_{\tau_{n+1}}$. Closest path option aligns with the shortest path distance, i.e., $\min \lambda_{\overrightarrow{ij}}$. A distance window is introduced, joining j in ζ_{τ_n} and i in $\mathbb{Z}_{\tau_{n+1}}$ based on $\lambda \leq \{250,500,...\Lambda\}$.*

Step 2.2. Benchmark index: *Rendering the simulation solutions in set ζ and χ into incidence matrices with same $n \times m$ features. Jaccard similarity coefficient (Φ), considering the intersection and union size ratio is applied, i.e., $J(\chi_{\tau_{n+1}}, \zeta_{\tau_{n+1}}) = |\chi_{\tau_{n+1}} \cap | / |\chi_{\tau_{n+1}} \cup \zeta_{\tau_{n+1}}|$. Resulting indexes split the U_B, L_B and scaled distance window.*

Input:

Initiate path options as $\mathbb{Z} = \begin{cases} class = \text{in-operation} \\ class = \text{cancelled} \end{cases}$

Subset $\mathbb{Z}$ to $\chi = \mathbb{Z}_{\tau_{n+1}}$ ▷ True disruption

Subset $\mathbb{Z}$ to $\zeta = \mathbb{Z}_{\tau_n}$ ▷ Pre-step basis

Introduce distance scale $\lambda \leq 250, 500, ..., \max \Lambda$

Output:

Estimate Φ as the cascading failures index with $0 \leq \Phi \leq 1$

Solve the L_B, U_B and distance window under λ

while $\tau_n \leq 22$ **do** ▷ Weekly range

  estimate on ζ next $n+1$ as U_B, L_B

    join $j_{\zeta_{\tau_n}}, i_{\mathbb{Z}_{\tau_{n+1}}}$ $\overrightarrow{ij} \forall \overrightarrow{IJ}, \min \lambda_{\overrightarrow{ij}} \subseteq \overrightarrow{IJ}$ ▷ Boundary range

    return ζ_{n+1}

    solve $\Phi = J(\chi_{\tau_{n+1}}, \zeta_{\tau_{n+1}})$

  for on $\lambda \leq \{250,500,...\Lambda\}$ **do** ▷ Distance window

    estimate on ζ next $n+1$ as window

    join $j_{\zeta_{\tau_n}}, i_{\mathbb{Z}_{\tau_{n+1}}}$ $\lambda \overrightarrow{ij} \subseteq \overrightarrow{IJ}$

    return ζ_{n+1}

    solve $\Phi = J(\chi_{\tau_{n+1}}, \zeta_{\tau_{n+1}})$

  end for

end while

interpreted as a recovery, due to waning COVID-19 infections starting in May or growing consumer spending driven by stimulus in the United States, remains speculative.

The global pandemic can be seen as a crisis with an exogenous origin, which imposed a sudden shock to liner shipping networks. However, the visual analysis does not indicate that the pandemic impaired the whole liner shipping network. This is similar to the findings of previous studies on maritime networks following the pandemic (March et al., 2021; Notteboom et al., 2021; Verschuur et al., 2021; Guerrero et al., 2022). The charts below show that the ratio between suspended to operational services hovered between 19.6% and 26.4% during the observation period (i.e., line graph). The operational services in the clusters (i.e., bar graph) point to the overall tendency that larger clusters were disproportionally impacted by blank sailings. Against this background, the pandemic can be characterized as a disruption along main trade route clusters with an origin in Intra-Asia trades and a relatively significant disruption in North America. This is because merchandise trade is primarily East-West, rather than North-South and important manufacturing hubs are situated in East Asia. As networks became increasingly distressed, the shock became visible in the United States given the country's high dependency on imports from China.

4.2. Network description

Recognizing that the disruption phases are systematic, we delineated between a pre-COVID phase in January 2020 and a pandemic disruption in the subsequent observations. Notwithstanding data limitations, our

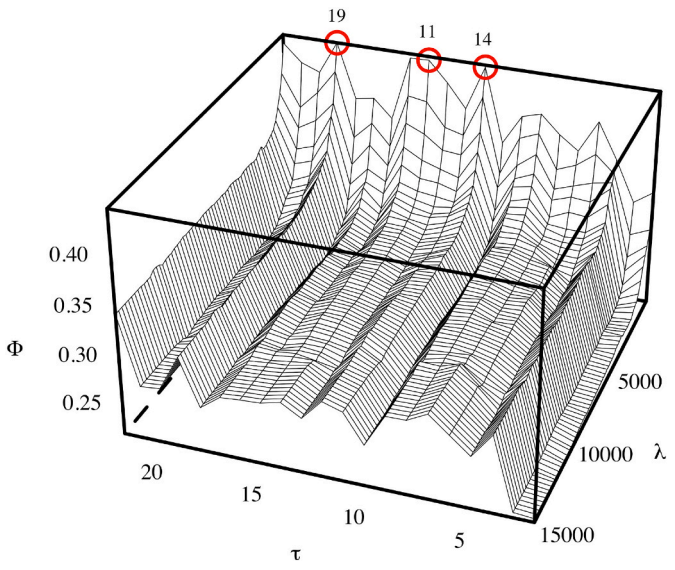

Fig. 4. Network simulation - Weekly instances τ_{1-22}. Note: Iterative approach with pre-step simulation basis in τ_n and a step-wise estimation considering the lower- (L_B), upper bound (U_B) and a scaled distance window. U_B equates to joining any matching voyage, i.e., $j_{\zeta_{\tau_n}} = i_{\mathbb{Z}_{\tau_{n+1}}}$. L_B equates to joining voyages via the shortest path distance, i.e., $min\lambda_{\overrightarrow{ij}}$. Distance window joining j in ζ_{τ_n} and i in $\mathbb{Z}_{\tau_{n+1}}$ based on $\lambda \leq \{250,500,\ldots,\Lambda\}$. λ expressed as nautical miles. Sets are benchmarked against χ using the Jaccard index (Φ), i.e., $J(\chi_{\tau_{n+1}}, \zeta_{\tau_{n+1}}) = |\chi_{\tau_{n+1}} \cap |/|\chi_{\tau_{n+1}} \cup \zeta_{\tau_{n+1}}|$.

work captures the shift along the initial pandemic phases. Table 2 outlines the network dynamic on a weekly basis for the period between 30th December 2019 and 31st May 2020. The available information for the months of January allowed us to benchmark disruption occurrences between the period before the effects of the pandemic became noticeable (i.e., *week* = {1, …, 4}, pre-COVID) and the following four months (i.e., *week* = {5, …, 22}). We argue that the disruption to the network in the early months of 2020 can be primarily attributed to seasonal distortions. Yet, it should be noted that a true benchmark (i.e., comparing operations under normal conditions with operations during the pandemic) would require multiple year-on-year network information.

In January 2020, on average, ≈114 vertices in the liner network were impacted; during the disruption, this number rose to ≈135 vertices, constituting a 18.6% increase. The pandemic disruption peaked in *week* 9 with 154 affected vertices, implying that 25% of the network endured distress. Another peak can be observed in *week* 22, although the overall operational network size diminished due to the suspended services. A similar pattern is observable in the number of the edges: in the '*normal*' phase, ≈316 links ($i \rightarrow j$) were disrupted, and in the pandemic phases, this grew to ≈417 links. This suggests that disrupted connections increased by 32.0%. Against this background, the network size measured by vertices was impacted to a lesser extent than the actual connectivity.

Meanwhile, there was a 5.8% decrease in the length of disrupted links (in nautical miles), comparing the '*normal*' and pandemic phases. In contrast, the operational links length dropped by just 1.9%. In conjunction with the significant difference in link length, it can be inferred that suspensions occurred foremost on long-haul services, with a slight tendency toward blanking shorter links. This observation is supported by the prior visual analysis, which highlighted the disruptions to the Pacific and Atlantic trades.

The network diameter was 14.5 in the pre-COVID phase, but diminished by 5.7% to $13.\bar{6}$ in the subsequent phases. This suggests that the disrupted network become more connected as the disruption propagated over time. In other words, the shortest path length between the most distant network nodes diminished, implying that a disruption propagation occurred that linked the network more tightly.

The average diameter value of the benchmark index for the whole observation period, considering the disrupted over the operational network, was ≈0.95, which indicates that the disrupted shortest distance between the most distant points aligns with the operational one. The beta index supports the insights provided by the diameter (i.e., the disrupted network becomes more connected), as well as indicates that the network includes several circuits. This latter point can be explained by the liner schedule design, with paths terminating in the source point. The gamma index, measuring the theoretical maximum connectivity (i.e., observed links and possible links), indicates that the disrupted network is far more connected than the undisrupted network.

The total degree centrality in the '*normal*' phase was, on average, ≈0.1 and grew by 33.2% to ≈0.13. This implies that the disrupted network's completeness rose (i.e., nodes sharing more links with other nodes in the network). In the same way, the benchmark against the operational network rose by 35.6% and reached an index above 1, on average, during the pandemic phases. Overall, this means that the disrupted network features a greater number of nodes sharing more links with other nodes in the network than does the operational network. The betweenness centrality shows a more moderate increase of 7.5% and, barring a few outliers, ranged above 1 in all observation points. On a graph level, this index displays that the average disrupted points within the network are more accessible (i.e., suggesting a possible stronger impact on hubs).

The global and local transitivity (i.e., overall clustering coefficient and average local clustering coefficient) grew respectively by 7.6% and by 19.0%. In light of this result, it is notable that the share of tightly connected communities increases when comparing the '*normal*' to the '*pandemic*' disruption network, and that clustering in the disrupted network is significantly higher than in the operational network. In contrast, local transitivity is lower in the disrupted network.

As a whole, the descriptive stage of the analysis indicates that the disruption impacted around one-fifth of the network: Mainly ocean voyages rather than short-sea operations. A more connected and complete disruption network hints at some degree of a disruption propagation. Finally, network clustering was significantly more present in the disrupted network than in the operational one. While the disruption imposed a strain on liner shipping operations and affected several links in the network, we cannot talk of a network breakdown (i.e., complete suspension of trade across macro-regions) on the basis of the data used. The liner shipping networks appeared extremely resilient.

4.3. Network failure simulation

While the descriptive stage highlighted a more connected and complete disruption network during the observation period, we were able to identify some disruption propagation. We propose a simulation-based benchmark index to shed further light on the disruption dynamic of cascading failures. Such failures spread through the system in response to a rare event (Dolgui et al., 2018). In maritime systems, these cascading failures constitute the ripple effect and are observed within geographical constraints, with points in the vicinity of the disruption source experiencing a shock that propagates along the network (Rousset and Ducruet, 2020).

We assessed the degree and condition (i.e., given λ as scaling variables) to which a disruption propagates step-wise in a sequence $i \rightarrow j$ and $j \rightarrow z$ through the network. This approach scales the distance to the initial node under distress in order to capture the geographical and time-variant disruption behavior. We specified the disruption's minimum and maximum reach on a direct link by defining a lower boundary (L_B) and an upper boundary (U_B). As indicated in Table 2, the underlying disruption (χ) is more similar to the L_B than the U_B, suggesting that the disruption spread in a geographically constrained manner. Given this observation, we conclude that, at a minimum, a local propagation

occurred. Along the observation horizon (τ), a slight upwards drift is visible, implying that χ converges with the simulated ripple effect behavior as more nodes in the system are impacted.

The use of a scaling variable allows some further observations. As shown in Fig. 4, for $\tau = \{11, 14, 19\}$ the similarity index peaks in mid-March, April and May. Such a pattern is consistent with a disruption propagation in March (i.e., shift from an Intra-Asia and Pacific trade to secondary clusters) and a resurgence of disruptions in May, which impacted almost all clusters. It is worth noting that the L_B was just crossed once in *week 4*, i.e., the actual disruption and the simulated disruption with a higher reach were more similar than the actual disruption and the lower bound (L_B) simulated disruption. Whether this is a statistical anomaly or relates to the initial shock in January's last week is difficult to assess. Overall, the index points to a propagation that unfolds at least locally, but does not seem to indicate an unmitigated spread throughout the liner shipping network.

5. Discussion

From the analysis presented above, we can infer that, despite its global nature, the pandemic (at least in its initial phases) has been a geographically-constrained disruption: A single local source spreading to a limited number of adjunct clusters within the liner shipping network. Some local disruption propagation altered network structures, resembling what has been described in theory as the ripple effect (Dolgui et al., 2020; Ivanov and Dolgui, 2021). A disruption that imposes contextual failures of a similar magnitude in various locations—rather than the more gradually intensifying shock from a specific geographical cluster like we observed—could have resulted in a much more impactful disruption, challenging whether liner shipping operators would have been able to prevent the collapse of the system. It can be argued that disruptions with local propagation enable the system to adapt to and cope with the adverse implications of the disruption. This seems to suggest that diversification and polycentric networks would work as a resilient approach to even more severe network disruptions.

As highlighted by the network size benchmark among undisrupted and disrupted services, the disruption impacted a limited portion of the global liner network, where between 19.6% and 26.4% of services (or between 17% and 25% of nodes in the network) were affected throughout the whole observation period. From this, we can presume that liner operators' response measures (e.g., service rescheduling and cancellation) mitigated the disruption's impact, providing a safeguard against a complete network breakdown. Canceled service commitments served as redundancies or so-called robustness reserves, enabling system flexibility and reducing the magnitude of the impact of the catastrophic event, in line with theory (Ivanov et al., 2014; Dolgui et al., 2018).

Overall, the pandemic's initial phases from January to May 2020 can be characterized foremost as a story about disrupted manufacturing hubs in East Asia and high trade dependency between Asia and North America. Other clusters, such as Europe, and trade hubs in West Asia and the Indian sub-continent also reported distress. Smaller North-South trades (i.e., Latin America and Africa) were impacted to a lesser extent, showing resilience to the global pandemic. As a consequence, this study indicates that, at least initially, the disruption was contained within some geographical dimensions.

It is interesting that some of the nodes most affected were not those in proximity of the source of disruption, but those characterized by high connectivity and lower call frequency. This seems to support the observation that trade dependence on a limited number of countries is a potential source of risk if those sourcing countries are affected by a network disruption. When comparing the impact of the network disruptions between Europe and North America, the former seems to possess a higher resilience in its maritime networks. Of course, it would be important to further test this observation by investigating the disruption dynamics in the later months of the pandemic.

From a broader perspective, the horizontal inter-organizational flexibility provided by strategic alliances within the liner shipping sector allowed firms to preserve some connectivity within the system, even in the wake of the health emergency and the widespread economic activity closures. As the analysis of the liner schedules indicated, operators introduced parallel services on key lanes or shared service codes.[4] These management practices, aimed at maintaining high capacity utilization levels, helped to minimize the liner operators' overcapacity, as suggested in the literature (e.g., Agarwal and Ergun, 2008, 2010) and in general fostered operational resilience. The more effective management of capacity, due to better collaboration, underpins the sector's surprisingly sustained earnings.

Additionally, it should be noted that the network failures resulting in the cluster disruptions followed a domino or snowball effect as predicted in the literature (Ivanov, 2017). That likely impacted not only the shipping sector, but also the hinterland transport networks. The worsening consequences with each ripple are likely to have resulted in higher inventory costs, re-bookings, loss of perishable goods, and a decline in customer satisfaction. Moreover, planning unreliability due to cancelled transportation services eroded trust between contract parties, although we expect that the global nature of the pandemic will have mitigated this erosion. Overall, this process might have reduced shippers' power over their own access to the transport network, which potentially ripples back to the operators and leads to lower revenues in the long-term.

Although the ripple effect was mostly observable at a cluster level during the initial phases of the pandemic, its implications are potentially far-reaching. In hindsight, it seems possible that the freight rate hike that started in the second half of 2020 might be the longer tail of the ripple effect, compounded by the impact of a longer pandemic duration. In fact, the mitigation efforts carried out by ocean carriers are likely to cause a longer-term capacity reduction due to carriers delaying investment in new tonnage and taking a conservative approach before increasing operational capacity. As economic activity accelerates, networks may slowly adapt to higher demand levels and their operational capacity may grow slowly in tandem.

6. Conclusions

Ocean shipping networks offer a useful illustration of how disruption dynamics propagate on a global scale. Reoccurring disruptions create an opportunity to draw insights (i.e., disruption magnitude, length, and frequency) from historical data, enabling the industry to anticipate and mitigate interruptions to operations. By contrast, the pandemic was an irregular occurrence with an exogenous origin, which proved to be a challenging event for the industry. The disruption simultaneously impacted health and economic systems in an unprecedented manner (Ivanov, 2020).

In this study, we used distress signals published by liner operators to quantify the pandemic disruption's initial degree and dynamic. Our work's theoretical contribution is that we assessed for the first time operational behavior under distress, highlighting disruption clustering and cascading failures in liner shipping networks. We showed how the pandemic imposed a gradually intensifying shock to some geographical clusters while operators tried to preserve network connectivity through a three-stage network analysis. We show that a local disruption propagation occurred, providing some empirical evidence to the cascading failures in ocean shipping networks. We argue that the suspended services by liner operators, which served as a risk mitigation strategy, eroded the contractual relationship with shippers by limiting the latter's control over their own access to the transport network. Our work should

[4] Based on the schedule sets (Linescape, 2020), this study estimates that an individual ship is managed on average by more than one operator firm (factoring out group holdings, such as CMA-CGM and APL, etc.) with the peak during February and March 2020. This finding implies that operators suspended services while maintaining connectivity through the alliance network.

generally encourage practitioners to identify robust responses to disruptions, especially as they become more frequent in an increasingly complex and globalized market environment.

Naturally, this work features some limitations. We narrowed our scope to operational responses (particularly service rescheduling and cancellation) in order to investigate the effect of the pandemic's disruption on network dynamics. Thus, future studies should investigate other aspects such as alternative routing, changing calling frequencies, or chartering operations. Second, our study is primarily of an exploratory nature, given the limited number of studies empirically investigating the liner shipping network dynamics as a result of the pandemic (which is still affecting a large portion of the world at the time of writing). In this respect, future studies could formalize our research's findings in a set of hypotheses that can be tested once more data on the pandemic becomes available. Research should investigate how the epidemiology of COVID-19 is correlated with network structures accounting for the different phases of the pandemic. Third, because of the complexity of liner shipping operations and the lack of capacity data, we did not account for capacity withdrawn due to suspended services; as a result, we could not include weights in the network analysis. One can argue that canceled service commitments should be measured in terms of withdrawn capacity rather than the number of services, even though most deep-sea services are likely to have similar weights. Moreover, we disregarded other cancellation reasons, which prevented us from solely attributing changes in stakeholders' behavior to the pandemic. Whether these additional inputs would result in an improved understanding of network dynamics and pandemic responses should be further investigated.

Future research can support the discussion on transport geography and the ripple effect, which may reveal how to prevent major disruptions in global trade networks. The paper proposes a simulation-based approach for identifying whether a cascading disruption is present within networks, but more robust methods such as Bayesian network or Markov chain models might yield further insights. In addition, scholars might examine the pandemic's implications on the power balance among supply chain partners. This could also include the analysis of hinterland network dynamics. Furthermore, maritime transport networks do not work in isolation, which warrants an investigation into intermodal network dynamics during a catastrophic incident.

Authors statement

Conception and design of study: C. Dirzka, M. Acciaro. Acquisition of data: C. Dirzka. Analysis of data: C. Dirzka. Interpretation of data: C. Dirzka, M. Acciaro. Drafting the manuscript: C. Dirzka. Revising the manuscript: C. Dirzka, M. Acciaro.

Appendix

Table 3
Cluster structure.

Cluster	UN/LOCODE Code
[1]	USEWR, USBAL, USMOB, USHOU, USMSY, USPEF, USBOS, USILM, USJAX, USPHL, BSFPO, CAMTR, USTPA, USMIA, USNYC, USCHS, USSAV, USORF
[2]	TRAMR, ITGIT, ITNAP, PTSIE, ITLIV, NLAMS, GBLIV, ESBIO, ESGIJ, ESVGO, PTLEI, RUKGD, SEGOT, MAPTM, TRYAR, TRTEK, MTMLA, FRDKK, MTDIS, ROCND, HRRJK, UAODS, DEBRV, SIKOP, ITTRS, MTMAR, BEZEE, PLGDN, DEWVN, TREYP, MATNG, ITSPE, ITGOA, TRIST, TRIZT, TRALI, ESBCN, DKAAR, BEANR, GBFXT, ESALG, ITVCE, GRPIR, DEHAM, ESTAR, ESVLC, FRLEH, GBLGP, GBSOU, NLRTM, FRFOS
[3]	PACTB, JMKIN, DOCAU, COCTG, ECGYE, PAONX, PAPCN, PAMIT, PAROD, COBUN, PABLB
[4]	RUVYP, CNLYG, JPOSA, CNFOC, CNZOS, JPYOK, KRINC, KRKWA, CNTXG, KRKAN, JPNGO, JPSMZ, JPUKB, TWKEL, CNNSA, KRUSN, JPTYO, TWTPE, CNDLC, CNFQG, CNTAO, HKHKG, CNNGB, CNSHA, CNSHK, CNXMN, KRPUS, TWKHH, CNYTN
[5]	OMSLL, SAKAC, ILHFA, EGPSE, EGAIS, QADOH, EGALY, SAJUB, LBKYE, LBBEY, AEKHL, EGPSD, EGEDK, DJJIB, SADMM, BHKBS, QAHMD, EGSUZ, JOAQJ, EGDAM, ILASH, TRMER, AEAUH, OMSOH, JOAQB, IQUQR, EGSCN, EGSOK, SAJED, AEJEA
[6]	INTUT, PKBQM, INNSA, PKKHI, INMUN, INMAA, INKAT, INPAV, LKCMB
[7]	MYPEN, IDSUB, IDJKT, MYPGU, MYLPK, VNTCG, THLCH, MYTPP, VNVUT, SGSIN, VNCMT, MYPKG
[8]	CLPAG, PECLL
[9]	MXLZC, MXVER, MXATM, MXZLO
[10]	CAPRR, MXESE, USTIW, USLGB, CAVAN, USOAK, USSEA, USLAX
[11]	NAWVB
[12]	TGLFW, BJCOO, GHTEM, CIABJ, NGAPP, NGLOS
[13]	ZADUR
[14]	VNHPH
[15]	TZDAR, KEMBA
[16]	CAHAL
[17]	CLCNL, CLLQN, CLSAI

References

Agarwal, R., Ergun, “O., 2008. Ship scheduling and network design for cargo routing in liner shipping. Trans. Sci. 42 (2), 175–196. https://doi.org/10.1287/trsc.1070.0205.

Agarwal, R., Ergun, ”O., 2010. Network design and allocation mechanisms for carrier alliances in liner shipping. Oper. Res. 58 (6), 1726–1742. https://doi.org/10.1287/opre.1100.0848.

Bank world, 2020. COVID-19 - signs of recovery? Trade Watch 6. https://documents1.worldbank.org/curated/en/188381593450101888/pdf/COVID-19-Trade-Watch-June-29-2020.pdf.

Bombelli, A., 2020. Integrators' global networks: a topology analysis with insights into the effect of the COVID-19 pandemic. J. Trans. Geogr. 87 (July), 102815. https://doi.org/10.1016/j.jtrangeo.2020.102815.

Borgatti, S.P., 2005. Centrality and network flow. Soc. Networks 27 (1), 55–71. https://doi.org/10.1016/j.socnet.2004.11.008.

Borkowski, P., Jażżdżewska-Gutta, M., Szmelter-Jarosz, A., 2021. Lockdowned: everyday mobility changes in response to COVID-19. J. Trans. Geogr. 90 (January), 102906. https://doi.org/10.1016/j.jtrangeo.2020.102906.

Brouer, B.D., Dirksen, J., Pisinger, D., Plum, C.E.M., Vaaben, B., 2013. The vessel schedule recovery problem (vsrp) - a mip model for handling disruptions in liner shipping. Eur. J. Operat. Res. 224 (2), 362–374. https://doi.org/10.1016/j.ejor.2012.08.016.

Bunge, W., 1966. Theoretical Geography. Gleerup, Lund.

Calatayud, A., Mangan, J., Palacin, R., 2017. Vulnerability of international freight flows to shipping network disruptions: a multiplex network perspective. Trans. Res. Part E: Logistics Trans. Rev. 108 (December), 195–208. https://doi.org/10.1016/j.tre.2017.10.015.

Chang, H.-H., Lee, B., Yang, F.A., Liou, Y.Y., 2021. Does COVID-19 affect metro use in taipei? J. Trans. Geogr. 91 (February), 102954. https://doi.org/10.1016/j.jtrangeo.2021.102954.

Chauhan, V.K., Perera, S., Brintrup, A., 2021. The relationship between nested patterns and the ripple effect in complex supply networks. Int. J. Prod. Res. 59 (1), 325–341. https://doi.org/10.1080/00207543.2020.1831096.

Christiansen, M., Fagerholt, K., Nygreen, B., Ronen, D., 2013. Ship routing and scheduling in the new millennium. Eur. J. Operat. Res. 228 (3), 467–483. https://doi.org/10.1016/j.ejor.2012.12.002.
Christiansen, M., Fagerholt, K., Ronen, D., 2004. Ship routing and scheduling: status and perspectives. Trans. Sci. 38 (1), 1–18. https://doi.org/10.1287/trsc.1030.0036.
Christiansen, M., Hellsten, E., Pisinger, D., Sacramento, D., Vilhelmsen, C., 2020. Liner shipping network design. Eur. J. Operat. Res. 286 (1), 1–20. https://doi.org/10.1016/j.ejor.2019.09.057.
Crucitti, P., Latora, V., Marchiori, M., 2004. Model for cascading failures in complex networks. Phys. Rev. E 69 (4), 045104. https://doi.org/10.1103/PhysRevE.69.045104.
[Dataset] Linescape, 2020. Sailing Schedule Data Solutions. Linescape. https://www.linescape.com.
[Dataset] Ocean Insights, 2020. Ocean Visibility At Its Best. Ocean Insights. https://www.ocean-insights.com.
De Vos, J., 2020. The effect of COVID-19 and subsequent social distancing on travel behavior. Trans. Res. Interdiscip. Perspec. 5 (May), 100121. https://doi.org/10.1016/j.trip.2020.100121.
DHL, 2021. Blank Sailing. https://lot.dhl.com/glossary/blank-sailing.
Dijkstra, E.W., 1959. A note on two problems in connexion with graphs. Numer. Mathemat. 1 (1), 269–271. https://doi.org/10.1007/BF01386390.
Dolgui, A., Ivanov, D., Rozhkov, M., 2020. Does the ripple effect influence the bullwhip effect? an integrated analysis of structural and operational dynamics in the supply chain. Int. J. Prod. Res. 58 (5), 1285–1301. https://doi.org/10.1080/00207543.2019.1627438.
Dolgui, A., Ivanov, D., Sokolov, B., 2018. Ripple effect in the supply chain: an analysis and recent literature. Int. J. Prod. Res. 56 (1), 414–430. https://doi.org/10.1080/00207543.2017.1387680.
Ducruet, C., 2013. Network diversity and maritime flows. J. Trans. Geogr. 30 (June), 77–88. https://doi.org/10.1016/j.jtrangeo.2013.03.004.
Ducruet, C., 2016. The polarization of global container flows by interoceanic canals: geographic coverage and network vulnerability. Maritime Pol. Manage. 43 (2), 242–260. https://doi.org/10.1080/03088839.2015.1022612.
Ducruet, C., 2020. The geography of maritime networks: a critical review. J. Trans. Geogr. 88 (October), 102824. https://doi.org/10.1016/j.jtrangeo.2020.102824.
Ducruet, C., Beauguitte, L., 2014. Spatial science and network science: review and outcomes of a complex relationship. Networks Spatial Econ. 14 (3), 297–316. https://doi.org/10.1007/s11067-013-9222-6.
Ducruet, C., Notteboom, T., 2012a. Developing Liner Service Networks in Container Shipping. https://halshs.archives-ouvertes.fr/halshs-00682949.
Ducruet, C., Notteboom, T., 2012b. The worldwide maritime network of container shipping: spatial structure and regional dynamics. Global Networks 12 (3), 395–423. https://doi.org/10.1111/j.1471-0374.2011.00355.x.
Ducruet, C., Rozenblat, C., Zaidi, F., 2010. Ports in multi-level maritime networks: evidence from the atlantic (1996–2006). J. Trans. Geogr. 18 (4), 508–518. https://doi.org/10.1016/j.jtrangeo.2010.03.005. Special issue on comparative north american and european gateway logistics.
Earnest, D.C., Yetiv, S., Carmel, S.M., 2012. Contagion in the transpacific shipping network: international networks and vulnerability interdependence. Int. Interac. 38 (5), 571–596. https://doi.org/10.1080/03050629.2012.726151.
Fleming, D.K., Hayuth, Y., 1994. Spatial characteristics of transportation hubs: centrality and intermediacy. J. Trans. Geogr. 2 (1), 3–18. https://doi.org/10.1016/0966-6923(94)90030-2.
Fransoo, J.C., Lee, C.-Y., 2013. The critical role of ocean container transport in global supply chain performance. Prod. Operat. Manage. 22 (2), 253–268. https://doi.org/10.1111/j.1937-5956.2011.01310.x.
Freeman, L.C., 1978. Centrality in social networks conceptual clarification. Soc. Networks 1 (3), 215–239. https://doi.org/10.1016/0378-8733(78)90021-7.
Gilmour, S., Yoneoka, D., Wang, Y., Dhungel, B., Li, J., Du, Z., Hao, Y., 2020. A bayesian estimate of the underreporting rate for COVID-19 based on the experience of the diamond princess cruise ship. https://doi.org/10.2471/BLT.20.254565. Preprint. nCoV.
Guerrero, D., Letrouit, L., Pais-Montes, C., 2022. The container transport system during COVID-19: an analysis through the prism of complex networks. Trans. Pol. 115 (January), 113–125. https://doi.org/10.1016/j.tranpol.2021.10.021.
Hartigan, J.A., 1975. Clustering Algorithms, 99th ed. John Wiley & Sons, Inc, USA.
Hotle, S., Murray-Tuite, P., Singh, K., 2020. Influenza risk perception and travel-related health protection behavior in the us: insights for the aftermath of the COVID-19 Outbreak. Trans. Res. Interdiscip. Perspec. 5 (May), 100127. https://doi.org/10.1016/j.trip.2020.100127.
Ito, H., Hanaoka, S., Kawasaki, T., 2020. The cruise industry and the COVID-19 outbreak. Trans. Res. Interdiscip. Perspec. 5 (May), 100136. https://doi.org/10.1016/j.trip.2020.100136.
Ivanov, D., 2017. Simulation-based ripple effect modelling in the supply chain. Int. J. Prod. Res. 55 (7), 2083–2101. https://doi.org/10.1080/00207543.2016.1275873.
Ivanov, D., 2020. Predicting the impacts of epidemic outbreaks on global supply chains: a simulation-based analysis on the coronavirus outbreak (COVID-19/SARS-CoV-2) case. Trans. Res. Part E: Logistics Trans. Rev. 136 (April), 101922. https://doi.org/10.1016/j.tre.2020.101922.
Ivanov, D., Dolgui, A., 2020. Viability of intertwined supply networks: extending the supply chain resilience angles towards survivability. A position paper motivated by COVID-19 outbreak. Int. J. Prod. Res. 58 (10), 2904–2915. https://doi.org/10.1080/00207543.2020.1750727.
Ivanov, D., Dolgui, A., 2021. OR-methods for coping with the ripple effect in supply chains during COVID-19 pandemic: managerial insights and research implications. Int. J. Prod. Econ. 232 (February), 107921. https://doi.org/10.1016/j.ijpe.2020.107921.
Ivanov, D., Sokolov, B., Dolgui, A., 2014. The ripple effect in supply chains: trade-off 'efficiency-flexibility- resilience' in disruption management. Int. J. Prod. Res. 52 (April) https://doi.org/10.1080/00207543.2013.858836.
Kosowska-Stamirowska, Z., 2020. Network effects govern the evolution of maritime trade. Proc. Nat. Acad. Sci. 117 (23), 12719–12728. https://doi.org/10.1073/pnas.1906670117.
Lam, Jasmine Siu Lee, Yap, W.Y., 2011. Dynamics of liner shipping network and port connectivity in supply chain systems: analysis on east Asia, journal of transport geography. Special Sec. Alter. Travel Fut. 19 (6), 1272–1281. https://doi.org/10.1016/j.jtrangeo.2011.06.007.
Li, C., Qi, X., Lee, C.-Y., 2015. Disruption recovery for a vessel in liner shipping. Trans. Sci. 49 (4), 900–921. https://doi.org/10.1287/trsc.2015.0589.
Li, C., Qi, X., Song, D., 2016. Real-time schedule recovery in liner shipping service with regular uncertainties and disruption events. Trans. Res. Part B: Methodol. 93 (November), 762–788. https://doi.org/10.1016/j.trb.2015.10.004. Maritime logistics.
Llaguno, A., Mula, J., Campuzano-Bolarin, F., 2021. State of the art, conceptual framework and simulation analysis of the ripple effect on supply chains. Int. J. Prod. Res. 1–23. https://doi.org/10.1080/00207543.2021.1877842, 0 (0).
March, D., Metcalfe, K., Tintoré, J., Godley, B.J., 2021. Tracking the global reduction of marine traffic during the COVID-19 pandemic. Nat. Commun. 12 (1), 2415. https://doi.org/10.1038/s41467-021-22423-6.
Mason, R., Nair, R., 2013a. Supply-side strategic flexibility capabilities in container liner shipping. Edit. Jingjing Xu Theo Notteboom. Int. J. Logistics Manage. 24 (1), 22–48. https://doi.org/10.1108/IJLM-05-2013-0053.
Mason, R., Nair, R., 2013b. Strategic flexibility capabilities in the container liner shipping sector. Prod. Plan. Control 24 (7), 640–651. https://doi.org/10.1080/09537287.2012.659873.
Notteboom, T.E., Vernimmen, B., 2009. The effect of high fuel costs on liner service configuration in container shipping. J. Trans. Geogr. 17 (5), 325–337. https://doi.org/10.1016/j.jtrangeo.2008.05.003.
Notteboom, T., Pallis, T., Rodrigue, J.-P., 2021. Disruptions and resilience in global container shipping and ports: the COVID-19 pandemic versus the 2008–2009 financial crisis. Maritime Econ. Logistics. https://doi.org/10.1057/s41278-020-00180-5. January.
Pesenti, R., 1995. Hierarchical resource planning for shipping companies. Eur. J. Operat. Res. 86 (1), 91–102. https://doi.org/10.1016/0377-2217(95)00063-V. EURO summer institute hierarchical planning.
Pooler, M., 2020. Shipping Lines Face Formidable Foe In Pandemic. Financial Times. https://www.ft.com/content/e9e69b0b-ae95-4f57-9a41-ea4f9756edd5.
Pooler, M., Hale, T., 2020. Coronavirus and Globalisation: The Surprising Resilience of Container Shipping. Financial Times. https://www.ft.com/content/65fe4650-5d90-41bc-8025-4ac81df8a5e4.
Qi, X., 2015. Disruption management for liner shipping. In: Lee, C.-Y., Meng, Q. (Eds.), Handbook of Ocean Container Transport Logistics: Making Global Supply Chains Effective. Springer International Publishing, Cham, pp. 231–249. https://doi.org/10.1007/978-3-319-11891-8_8. International Series in Operations Research & Management Science.
Rousset, L., Ducruet, C., 2020. Disruptions in spatial networks: a comparative study of major shocks affecting ports and shipping patterns. Networks Spatial Econ. 20 (2), 423–447. https://doi.org/10.1007/s11067-019-09482-5.
Saul, J., 2020. Shipping Lines, Ports Count Cost as Coronavirus Hits Supply Chains. Reuters. https://www.reuters.com/article/us-china-health-shipping-idUSKBN20E2GN.
Sobieralski, J.B., 2020. COVID-19 and airline employment: insights from historical uncertainty shocks to the industry. Trans. Res. Interdiscip. Perspec. 5 (May), 100123. https://doi.org/10.1016/j.trip.2020.100123.
Sokolov, B., Ivanov, D., Dolgui, A., Pavlov, A., 2016. Structural quantification of the ripple effect in the supply chain. Int. J. Prod. Res. 54 (1), 152–169. https://doi.org/10.1080/00207543.2015.1055347.
Suau-Sanchez, P., Voltes-Dorta, A., Cugueró-Escofet, N., 2020. An early assessment of the impact of COVID-19 on air transport: just another crisis or the end of aviation as we know it? J. Trans. Geogr. 86 (June), 102749. https://doi.org/10.1016/j.jtrangeo.2020.102749.
Tang, L., Jing, K., He, J., Stanley, H.E., 2016. Complex interdependent supply chain networks: cascading failure and robustness. Phys. A: Stat. Mech. Appl. 443 (February), 58–69. https://doi.org/10.1016/j.physa.2015.09.082.
United Nations, 2021. COVID-19 and Maritime Transport Impact and Responses. Transport and Trade Facilitation, no. 15: 77.
UNSDG, 2020. A UN Framework for the Immediate Socio-Economic Response to COVID-19. https://unsdg.un.org/resources/un-framework-immediate-socio-economic-response-covid-19.
Verschuur, J., Koks, E.E., Hall, J.W., 2021. Global economic impacts of covid-19 lockdown measures stand out in high-frequency shipping data. PLOS ONE 16 (4), e0248818. https://doi.org/10.1371/journal.pone.0248818.
Verschuur, J., Koks, E.E., Hall, J.W., 2020. Port disruptions due to natural disasters: insights into port and logistics resilience. Trans. Res. Part D: Trans. Environ. 85 (August), 102393. https://doi.org/10.1016/j.trd.2020.102393.
Wang, J., Du, D., Ma, L., 2021. Geovisualizing cancelled air and high-speed train services during the outbreak of COVID-19 in China. J. Trans. Geogr. 103002. https://doi.org/10.1016/j.jtrangeo.2021.103002. February.
Wang, S., Meng, Q., 2012. Liner ship route schedule design with sea contingency time and port time uncertainty. Trans. Res. Part B: Methodol. 46 (5), 615–633. https://doi.org/10.1016/j.trb.2012.01.003.

Wang, Y., Cullinane, K., 2016. Determinants of port centrality in maritime container transportation. Trans. Res. Part E: Logistics Trans. Rev. 95 (November), 326–340. https://doi.org/10.1016/j.tre.2016.04.002.

WHO, 2020. WHO Timeline - COVID-19. https://www.who.int/news/item/27-04-2020-who-timeline-covid-19.

World Economic Forum, 2020. Managing COVID-19: How the Pandemic Disrupts Global Value Chains. https://www.weforum.org/agenda/2020/04/covid-19-pandemic-disrupts-global-value-chains.

Wu, D., Wang, N., Yu, A., Wu, N., 2019. Vulnerability analysis of global container shipping liner network based on main channel disruption. Maritime Pol. Manage. 46 (4), 394–409. https://doi.org/10.1080/03088839.2019.1571643.

Wu, J.J., Gao, Z.Y., Sun, H.J., 2007. Effects of the cascading failures on scale-free traffic networks. Phys. A: Stat. Mech. Appl. 378 (2), 505–511. https://doi.org/10.1016/j.physa.2006.12.003.

Yu, D.K., Sophie, 2020. As China Returns to Work, It Is Hardly Business as Usual. Reuters. https://www.reuters.com/article/us-china-health-return-idUSKBN2020AL.

Zheng, H., Hu, Q., Yang, C., Chen, J., Mei, Q., 2021. Transmission path tracking of maritime covid-19 pandemic via ship sailing pattern mining. Sustainability 13 (3), 1089. https://doi.org/10.3390/su13031089.